Biol. Cybern. 75, 29–36 (1996)

Biological Cybernetics


# A model of the cerebellum in adaptive control of saccadic gain

## II. Simulation results

**Nicolas Schweighofer[1,2], Michael A. Arbib[1], Peter F. Dominey[3]**

[1] Center for Neural Engineering, University of Southern California, Los Angeles, CA 90089-2520, USA
[2] ATR Human Information Processing Research Laboratories, 2-2, Hikaridai, Seika-cho, Soraku-gun, Kyoto 619-02, Japan
[3] INSERM Unit 94, 16 ave du Doyen Lepine, F-69500 Bron, France

Received: 25 November 1994/Accepted in revised form: 6 February 1996

**Abstract.** A large, realistic cerebellar neural network has been incorporated into a previously developed saccade model. Using this model, in the present paper, we simulate the complex spatiotemporal behavior of the neuronal subpopulations implicated in adaptive saccadic control. Our simulation results are in good agreement with neurophysiological and behavioral data. Furthermore, we suggest several new experiments to test the validity of our predictions on adaptive saccadic control.

### 1 Introduction

The saccade generation model developed by Dominey and Arbib (1992) (henceforth referred to as the D&A model) takes into account many brain regions involved in the generation of saccades in the monkey. The primary goal of this model was to comply with the well-known anatomy and neurophysiology of the saccade system in simulating a variety of saccade paradigms. This model, however, does not include the cerebellum. In the companion paper (Schweighofer et al. 1996) we developed a cerebellar neural network of neural-like units to augment the D&A model, in order to account for the adaptive capabilities of the saccadic system.

We simulated the model in two phases. First we studied the real-time behavior of the model and notably the input/output of the cerebellum, with the aim of reproducing semirealistic neurophysiological data. We also made sure that the error detector model is appropriate, that is that it could induce cerebellar long-term depression (LTD) and could properly tune the saccadic system [we refer the reader to Schweighofer et al. (1996) for a complete description of the model and its biological substrate]. Second, once these 'per trial' experiments were shown to work, we ran adaptive simulations: over trials, the model had (1) to compensate for the nonlinearities of the saccadic system and (2) to show proper adaptation in the target perturbation experiment (Goldberg et al. 1993). The Appendix gives all the constants used in the simulations, including constant weights and initial setting of variable parameters. The model is implemented in the Neural Simulation Language NSL (Weitzenfeld 1991) on a Sun Sparc 10.

### 2 Neuronal responses

Figure 1 shows the input behavior of the cerebellar model in its 'naive state' in response to a target displacement of 23.75° to the right (the eye position is shown in Fig. 2).[1] Responses of individual cells from the three mossy fiber classes – visual (top), burst (middle) and tonic proprioception (bottom) – are shown. The visual mossy fibers, or long lead burst mossy fibers, fire before the saccades and terminate toward the end of the saccade: their activities are not directly proportional in size and/or duration to the size of the saccade. Since the visual mossy fibers are retinotopically coded, each fires only for similar saccades. The cell shown in Fig. 1, for instance, participates in the computation of the first saccade but not in the computation of the corrective saccade. Mossy fibers with very similar responses have been recorded by Kase et al. (1980). The second response displayed (Fig. 1, bottom) is the average response of short lead burst mossy fibers. The activity onset and duration of the burst are correlated with saccade onset and

*Correspondence to:* N. Schweighofer, ATR Human Information Processing Research Laboratories, 2-2, Hikaridai, Seika-cho, Soraku-gun, Kyoto 619-02, Japan (Tel: +81 774 95 1084, Fax: +81 774 95 1008, e-mail: nicolas@hip.atr.co.jp)

[1] For computational tractability, the visual input is discretized in step of 4.75°, so that the saccades that the model generates are 4.75°, 9.5°, 14.25° etc. Also, for an easier comparison between experimental results and simulation results, please note that the unit of time used in the simulation is 1 s

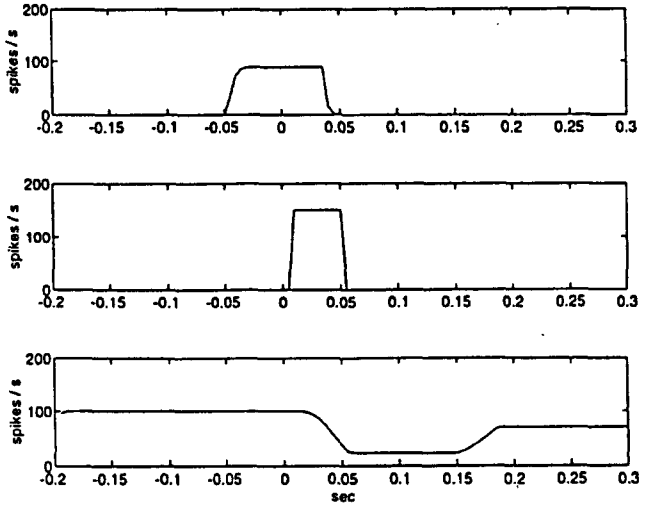


**Fig. 1.** Mossy fiber inputs to the cerebellum: From *top* to *bottom*: Average response for a visual (long lead burst) mossy fiber, response for a short lead burst mossy fiber response, and response for a tonic proprioceptive mossy fiber. The corresponding eye position is shown in Fig. 2, and $t = 0$ s corresponds to the onset of the saccade. The recorded visual mossy fiber fires strongly between $-0.5$ s and 0.05 s. The short lead burst mossy fiber fires strongly between 0 s about and 0.05 s. The tonic proprioceptive mossy fiber firing rate fires strongly when the eye is close to 0° (duration of the simulation 0.5 s)

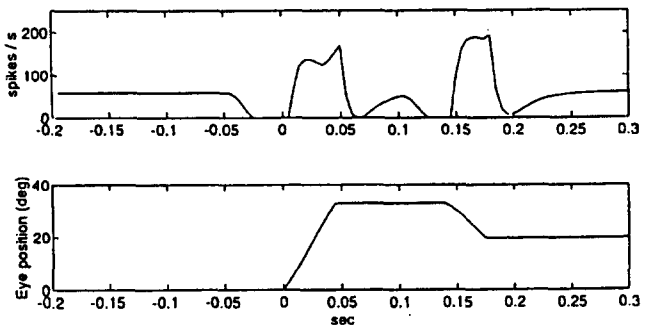


**Fig. 2.** Fastigial oculomotor region (FOR) cell responses. *Above*: Response of the right FOR cell before learning. *Below*: Eye position generated by the model before learning in response to a target displacement of 23.5° to the right. The eye first overshoots and then undershoots the target. Since the left FOR response (not shown) is very similar to the right FOR response, the total influence of the cerebellum on the final saccadic circuitry is minimal before learning (duration of the simulation 0.5 s)

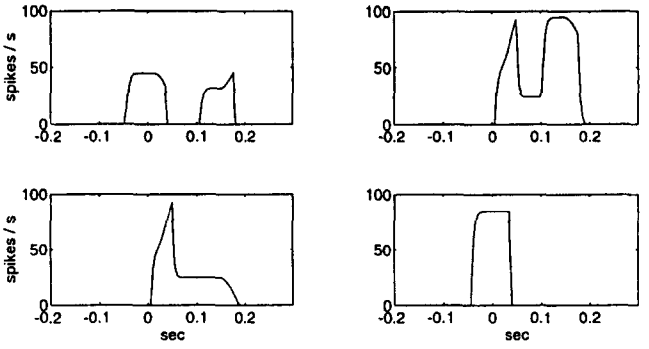


**Fig. 3.** Simulation of granule cell activity. Examples of four granule cell firing rates, picked randomly. Due to the random connection from the mossy fibers to the granule cells, the granule cell population carries a very rich combination of inputs. Therefore their responses can be trimodal (*top right*), bimodal (*top left* and *bottom left*) or unimodal (*bottom right*). They can fire for the main saccade and the corrective saccade (*top*) or for one saccade only (*bottom*)

amplitude, respectively. The short lead burst mossy fibers we modeled are directionally tuned so that the cell does not fire for the corrective saccade (both directional and nondirectional burst neurons have been reported by Kase et al.). The last mossy fiber display shows a proprioceptive tonic fiber which reflects the eye position change with fidelity (within its range). Such neurons, in addition to burst-tonic proprioceptive neurons, have also been recorded by Kase et al. (1980).

Fastigial oculomotor region (FOR) cell mean firing rates during saccades are displayed in Fig. 2. The upper graph shows the simulation of the right FOR cell, while the corresponding eye position with a main and a corrective saccade is shown in the lower graph. The FOR cell responses recorded by Fuchs et al. (1993) present many similarities with the model responses: (1) The FOR response is not direction specific, as firing occurs for the main saccade to the right and for the corrective leftward saccade. (2) The duration of the burst, but not its maximal activity, is correlated with the duration of the saccade (this is especially clear in the upper panel of Fig. 2). (3) There is no direct relation between eye position and firing rate as the maximum activity is influenced by Purkinje cell (PC) inhibition, which depends on previous learning. (4) The burst can be preceded by a pause and/or followed by another pause. It should be noted that result (1) is at odds with the results of Ohtsuka and Noda (1990), who recorded direction-selective FOR neurons. The pauses are created by early and late PC inhibition: as learning progresses the PC inhibition is somewhat reduced, and the pause may disappear.

The granule cells, due to their random connections to the mossy fibers, show diverse responses, as shown with the four examples in Fig. 3 (the eye displacement is the same as shown in Fig. 2). The signal they carry is either unimodal (bottom right), bimodal (top left and bottom left) or even trimodal (top right). Moreover, they can fire for one saccade only (bottom) or for two saccades (top). Very few recordings of granule cells have been made, and none have been made in the oculomotor system to our knowledge; however, given these results we expect them to appear to be quite random to the experimenter. Because our cerebellar model does not incorporate any cerebellar interneurons, and due to the simplification we made by taking only one PC per microcomplex, the PC responses do not reproduce any data. Understanding their individual responses would necessitate a careful analysis of the topology of the mossy fiber–granule cell–PC inputs, which is made difficult by the lack of data. Moreover, PC recordings (Kase et al. 1980; McElligot and Keller 1982) have shown such complex modulations of discharge that it is very difficult to relate the patterns to specific saccade metrics.

Figure 4 shows the functioning of the inferior olive (IO) as an error detector. Because the primary saccade is erroneous, the 'goal' neuron fires until the second saccade is over. The 'memory' neuron fires at the end of the saccade. Due to the activity of the 'memory' neuron, the pre-IO neuron fires after the first saccade is completed. When the corrective saccade is generated, the IO spikes with a probability proportional to the corrective saccade amplitude. If the first saccade was accurate, the 'goal' neuron would stop firing at the end of the saccade, before the 'memory' neuron would start to fire; because co-activation of both neurons is necessary for the pre-IO to fire, the pre-IO neuron would not fire. Therefore, the IO would be gated and would not fire.

A hypothesis underlying the model is the near synchrony of the peak concentration of the second messenger with the climbing fiber spike. Figure 5 allows the comparison between the timing of the peak of the total second messenger produced by the first saccade and IO spike occurrence. The first display in Fig. 5 shows the sum of all the granule cell activities for the first and corrective saccades. The second display (Fig. 5, middle) represents the total molarity of the second messenger in the 'left' PC over time produced by the first saccade *only*. The last display (Fig. 5, bottom) shows the timing of the 'left' IO spike triggered by the leftward corrective saccade. The spike occurs close to the peak of the second messenger activity, and therefore produces a large decrease in the efficacy of the synapses which participated in the first saccade. As discussed above, we chose to activate the IO by a motor error which stems from proprioceptive inputs. By comparing eye position (Fig. 2, bottom) and the IO response, we see that the IO spikes toward the end of the corrective saccade. If a visual error were implemented in the model, the IO would spike sooner, between $t = 0.1$ s and $t = 0.15$ s, with a visual feedback delay of 40–80 ms. Figure 5 (top) shows that the total granule cell activity which corresponds to the second saccade rises rapidly at $t = 0.1$ s. Hence, our concept of window of eligibility would still apply in the case of a visual error.

Figure 6 shows the activity of the FOR cells after learning the nonlinearities (see below). The display

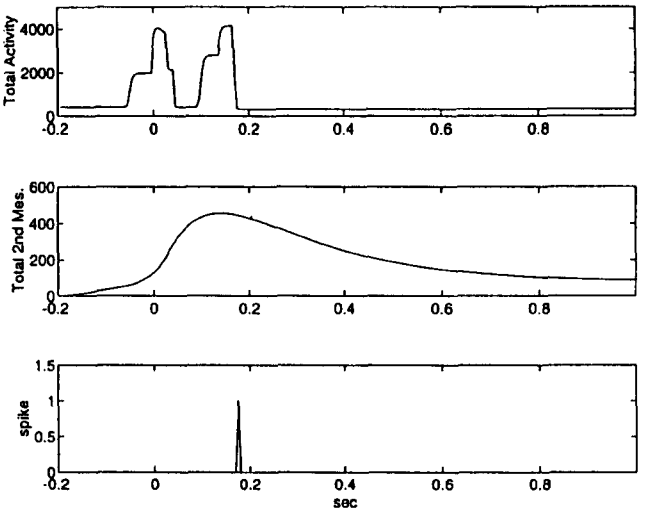


**Fig. 5.** Temporal aspects of the learning mechanism. Duration of the simulation 1.2 s, same eye displacement as in Fig. 2. *Top*: Total granule cell activity in the cerebellar cortex for the main and the corrective saccade. *Middle*: Total second messenger molarity released in 'left' Purkinje cell (PC) by the *first saccade only*. *Bottom*: 'left' IO spiking activity. Note that the second messenger molarity peaks close to the occurrence of the IO spike

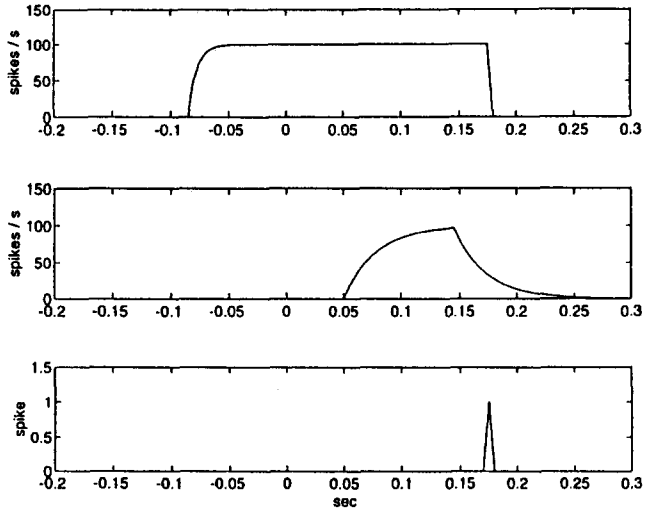


**Fig. 4.** Simulation of the inferior olive (IO). From *top* to *bottom*: Goal neuron mean firing rate, pre-IO neuron mean firing rate, IO spiking activity. Because the primary saccade is erroneous, the pre-IO neuron fires: this causes the ungating of the IO cells. When the corrective saccade is generated, the appropriate IO cell spikes since it can now receive phasic activity from the appropriate stretch receptor. Without a corrective saccade, the IO would be gated and would not fire

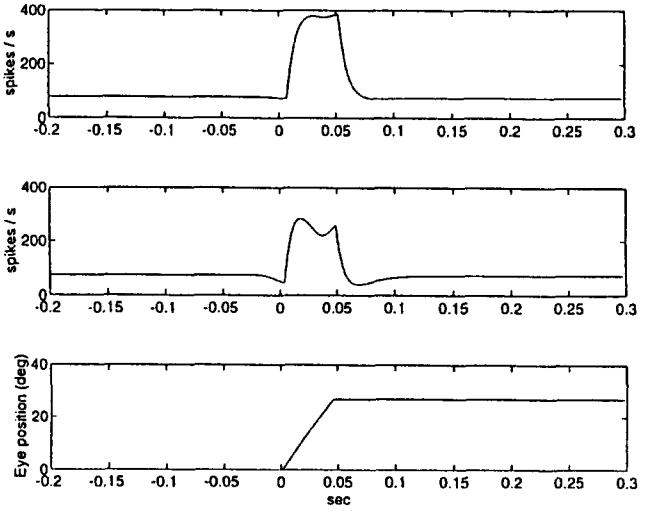


**Fig. 6.** FOR responses and eye position after learning of the proper saccadic gain (duration of the simulation 0.5 s). *Top*: Left FOR cell response. *Middle*: Right FOR cell response. *Bottom*: Corresponding eye position. No corrective saccades are generated. Due to the competitive mechanism, the difference in the FOR bursts generates the corrective signal issued by the cerebellum. Notice how the presaccadic and postsaccadic pauses have either disappeared or have been reduced

shows, respectively, the leftward FOR cell response (top), the rightward FOR cell response (middle) and the corresponding eye position (bottom). As the gain was greater than 1 before learning, leftward corrective saccades were generated during learning. This resulted in a decrease of the weights in the leftward PC and a release of excitation in the underlying FOR cell. In contrast, the rightward FOR neuron showed little increase in activity compared with before learning. Due to the competition between the two cells, the saccade now has the proper gain. Notice how the pauses disappeared totally for the leftward FOR cell and are somewhat reduced in the rightward FOR (compare with Fig. 2). Not all the neurons recorded by Fuchs et al. (1993) showed pauses, and many paused either after or before the burst. Our model shows that these authors could have recorded from only one population of FOR cells: our results suggest that the pauses are due to a stronger PC inhibition.

## 3 Learning experiments

We first trained the network to learn the nonlinearities of the system in order to obtain a unitary gain for all saccade amplitudes for all initial positions. We then performed the target perturbation experiments, with the set of weights we derived from the previous experiment. Figure 7 shows the gains for different saccade amplitudes (to the right) at different stages of learning. The upper (dotted) curve shows the gains before learning (or, equivalently, with a lesioned cerebellum, as the FOR has no influence on the final machinery at this stage). Note that, due to the relative randomness of the weights in the graded brainstem saccade generator masks, the gain for 19° saccades is larger than for 14.25°. We first trained the network to reduce the gain for small rightward and leftward saccades only (4.75°, 9.5°, 14.25° saccades, generated randomly) in order to reduce the oscillatory behavior, as the gain for these saccades is very large. The dash-dotted curve in Fig. 7 shows the gain of the system after 500 saccades. We then randomly generated 500 more rightward saccades of any amplitude (dashed curve) and then another 500 rightward saccades (continuous curve); at this later stage, no more corrective saccades were generated and thus this is the best learned state. Taken together, these different curves show how, over the course of learning, the gain converges towards 1 for all saccade amplitudes. When learning is completed, the gain actually reaches values very close to 1 for large saccades (the results are not as good for smaller saccades due to the relatively large discretization error). It is interesting to note that the curve corresponding to 1000 trials (dashed curve) shows a gain smaller than 1 in its middle range, and actually smaller than the gain for 1500 trials (continuous curve) for the similar saccade amplitudes. This phenomenon is due to the generalization process, as the control of middle range saccades uses common synapses with smaller and larger saccades (especially since all saccades are generated from 0° in this experiment). Consequently, the corresponding synaptic efficacies are decreased too rapidly. It takes more trials to 'ungeneralize'. While performing learning on saccade amplitudes only from the 0° initial position, we measured the saccadic gain for saccades starting from different initial positions. Figure 8a and b show the gain for 9.5° and 19° rightward saccades respectively, starting from different initial positions after 500, 1000 and 1500 trials. It is remarkable that the gain converges towards 1, even though the system is not trained specifically on these saccades. Thus, due to the important generalization process, after training on different saccade amplitudes from the 0° position, the network is well tuned to generate accurate saccades of any amplitude, from any initial position.

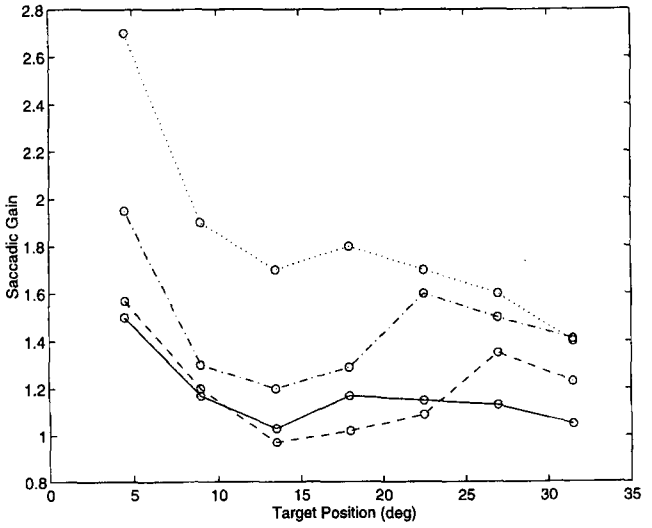


**Fig. 7.** Saccadic gain for different rightward saccades from the 0° initial position during learning. *Dotted curve*, saccadic gain before learning, or equivalently after cerebellar lesion; *dash-dotted curve*, after 500 'small' saccades randomly generated (left or right); *dashed curve*, after 500 more saccades of any amplitudes (to the right); *continuous curve*, after 500 more saccades of any amplitude (to the right). At this stage no corrective saccades are generated. Note how the gain converges towards 1 (the error for small saccades is due to the relatively large discretization)

Figure 9 shows the learning curve which reproduces the saccadic adaptation experiment. In this case, the primary target displacement of 23.75° is followed by a correction of 13.25°. The process reaches an asymptote after 250 trials, when corrective saccades are no longer generated. At 300 trials, the target is no longer perturbed, and re-learning occurs. The fuzziness of the curve is due to the probabilistic firing of the IO. The 'angle' visible in the learning curve around 19° is caused by the discretization of the visual input: as the error is proportional to the amplitude of the corrective saccades, which take only finite values, the learning is not as smooth as with the biological system, which is quasi-continuous due to the very fine visual resolution. In accordance with the behavioral data (Schweighofer et al. 1996, Fig. 2 left; M. E. Goldberg, personal communication), re-learning occurs faster. The nonspecific long-term potentiation (LTP) present in the model (implemented with weight normalization) is the reason for this phenomenon for the following reason:

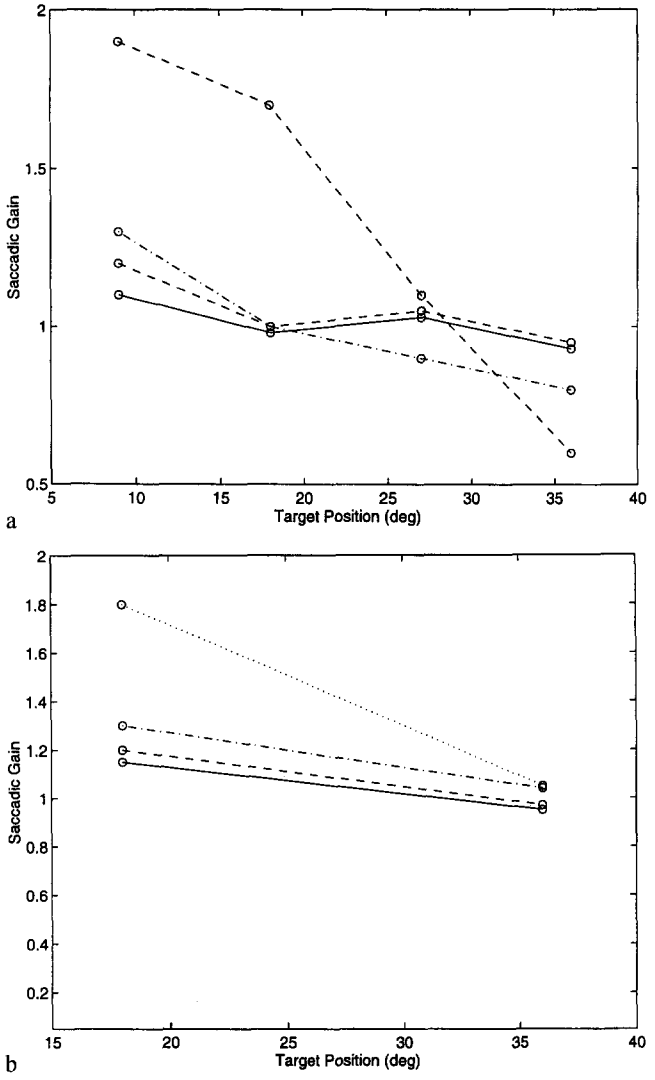


**Fig. 8.** Saccadic gain for different saccades from different initial positions: **a** 9.5° saccades, **b** 19° saccades. The gains are measured while performing the learning experiments shown in Fig. 7. It is the generalizing capabilities of the model which allows learning of these gains without specific training

Most of the synapses participating in the computation of the saccades generated during re-learning do not participate in the computations which correspond to learning since the directions of the saccades are different. Consequently, these synapses have seen their weights increased by LTP during the 250 first trials. Referring to (11) in Schweighofer et al. (1996) we see that the concentration of diacylglycerol released will be higher on average in these synapses at the beginning of the re-learning phase than in the synapses participating in the learning phase. Given that the weight change is proportional to the second messenger concentration when the IO spikes, re-learning occurs faster. Finally, note that the experimental curve, unlike the simulated learning curve, is noisy. The reason is that the brainstem saccade generator uses a 'noisy integrator', so completion of the saccade does not guarantee that the eye is on target. In the D&A

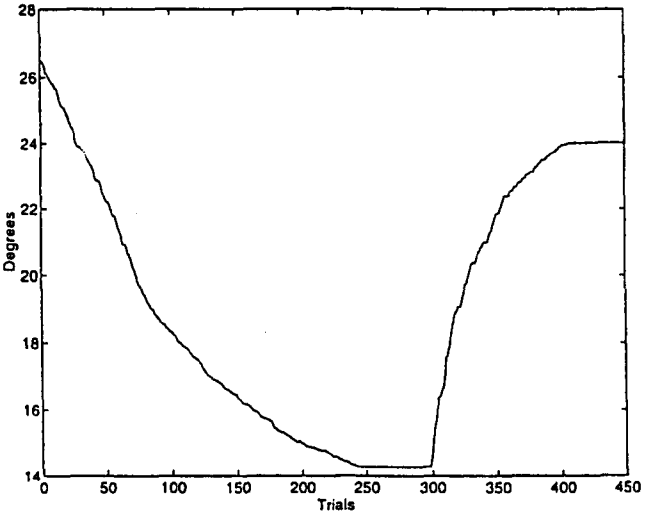


**Fig. 9.** Learning of the target perturbation experiment. Eye position (in degrees) is plotted against the number of trials. The primary target displacement of 23.75° is followed by a correction of 13.25°. Note (1) the non-constant decrease of the learning rate due to the probabilistic firing of the climbing fiber system and (2) the faster re-learning, similar to what happens in the experiments. Compare with the experimental data shown in Fig. 2 of Schweighofer et al. (1996)

model, there is no such variability of the response since no noise is added.

## 4 Discussion

### *4.1 Predictions derived from the study*

Available anatomical, neurophysiological, neurochemical and behavioral data on the cerebellar control of the saccadic system served to provide constraints to our model, and in order to accommodate many of these data we made a number of assumptions (Schweighofer et al. 1996). Given our successful results of simulation of the model in the present paper, we make the following predictions.

1) We predict that the cerebellum gradually learns part of the inverse model of the plant: the non-adaptive pathway is an approximate inverse model (which can be thought of as genetically programmed) which is being adaptively compensated for by the cerebellum.
2) In order for the cerebellum to effectively modify motor commands, we predict that only mossy fibers arising from the EBN give collaterals to the FOR. If the nuclear cell excitation were derived mainly from visual signals, temporal mismatches would not allow good saccadic control by the cerebellum.
3) We predict that, because of the unidirectional functional change in synaptic efficacies due to LTD, projections to both the inhibitory and excitatory burst neurons (IBNs and EBNs) are necessary to control the saccadic system.
4) In Schweighofer et al. (1996) we proposed a new neural model of the IO which gates the adaptation when needed. We predict that the error signal should

be 'directed' to the appropriate cerebellar microzone. Moreover, the poorly informative (binary) error signal is sufficient for learning to occur.

5) Taking into account the significant delay between the efferent motor command and the afferent error information, we predict that the cerebellar learning rule, based on neurochemical studies of LTD, should include a delayed memory term ('window of eligibility'). In the monkey or human it is often the case that the latency of a corrective saccade is up to 200–300 ms. The model is able to cope with such long latencies, as shown in Fig. 5 (middle): the second messenger is still present in important quantities in the PC synapses, even 300 ms after the saccade is completed. Since the weight change is proportional to the second messenger concentration, adaptation still occurs, albeit slower than with a latency of 150 ms. We also predict that even if there is 200 ms delay in presenting a step-back, target adaptation still occurs. In this case, the total delay is approximately 400 ms, and Fig. 9 shows that there is still a significant amount of second messenger present in the synapses. The prediction is that the adaptation is still going to happen, but more trials should be required.

While predictions 1 and 3 are difficult to verify experimentally, careful anatomical tracing could confirm prediction 2. Moreover, experiments can be designed to verify predictions 4 and 5, as discussed below.

### *4.2 Proposed experiments and extensions of the model*

In the present model, each IO cell fires in a binary manner, but with a probability which correlates with the amplitude of the error. This allows us to generate learning curves comparable to the real learning curves, i.e., with a smooth exponential-like decrease. In addition, the climbing fiber firing pattern over a number of trials is similar to that found by Gilbert and Thach (1977), i.e., the number of spikes decreases as adaptation occurs. Such recording of complex spikes would validate the model and give strong support to the Marr-Albus theories. Our model does not give an answer on the nature of the error carried by the climbing fibers, and leaves this as an open question that more experiments should resolve. To our knowledge, climbing fiber activity has not been seen in correlation with saccades and, as Houk et al. (1992) pointed out, the climbing fiber inputs to saccade-related regions of the cerebellar cortex remains somewhat of a mystery. In any case, more work at both the experimental and theoretical levels is needed to understand the nature of the error as well as the respective roles of the proprioceptive and visual inputs to the oculomotor region of the IO.

The concept of eligibility appears to be fundamental in trying to understand memory formation in the brain. In biological systems there are significant delays involved between an action and its consequences. Here, we have shown that for a system which has relatively long delays between the efferent command signal and the feedback error, a pure eligibility decay is not optimal. Instead a window of eligibility allows efficient learning. Since the activation of metabotropic receptors leading to diacylglycerol activation is a much slower process than the activation of AMPA receptors, it is indeed possible that the diacylglycerol concentration peaks when the error signal arrives. Careful recordings and analyses of the timing of the granule cell and IO cell activities, coupled with kinetics analysis of the different chemical factors playing a role in the induction of LTD for various systems, would be helpful for constructing a general theory on the role of the cerebellum in adaptive movement control. To know the time course of eligibility and further validate this model, an interesting behavioral experiment would be the following. In a modified target perturbation experiments, the target would be displaced a second time. In other words, while the monkey or the human subject is making the corrective saccade, the target would be perturbed again. The two learning curves that such an experiment would provide (one for the first saccade, the other for the second saccade) would give us more details on the time course of eligibility. A particularly interesting case would be to move the target in the opposite direction each time, with the third displacement larger than the second. It remains to be seen if a 'tug of war' would occur in the adaptation of the first saccade or not.

The present model gives realistic neuronal responses from these classes of mossy fibers and one class of FOR cells. However, the real cerebellum is much more sophisticated. In particular, the dual inputs from the cerebral cortex (this paper) and the superior colliculus (Houk et al. 1992) to the oculomotor vermis should be further analyzed by future experiments and integrated in a new model. As Lewis and Zee noted (1993), the observation that many of the cells within the oculomotor cerebellum that discharge in relation to saccades suggests the hypothesis that the critical shaping of the final portion of the saccade trajectory is a cerebellar function. This might be linked to the projections to the omnipause neurons, and more generally to the control of oblique saccades by horizontal and vertical brainstem saccade generators. Interesting implications as to how the cerebellum is involved in temporal coordination of motor pattern generators are likely to emerge from a study of these cerebellar projections to the omnipause neurons. Further extensions of the model would also include direction-specific dysmetria and floccular control of the tonic component of the saccade.

## **Appendix.** *Parameters used in the simulations*

The numerical values given here correspond to the cerebellar model only. For values of the whole saccade model refer to Dominey (1993).

*Number of neurons and number of synapses per neuron*

| | |
|---|---|
| 40 mossy fibers (mf) (19 visual + 11 proprioceptive + 10 EBN feedback) | 9 FEF → mfret synapses, 1 proprioception → mfpos synapses, 1 EBNr → mfburst synapse |

| | |
|---|---|
| 1000 granule cells (gc) | 4 mf → gc synapses |
| 2 Purkinje cells (pc) | 1000 gc → pc synapses |
| 2 nuclear cells (nuc) | 1 pc → nuc synapse, 1 EBN → nuc synapse |

*Time constants*

| | |
|---|---|
| Mossy fibers | $\tau_{mf} = 10$ ms |
| Granule cells | $\tau_{gc} = 6$ ms |
| Purkinje cells | $\tau_{pc} = 20$ ms |
| Nuclear cells | $\tau_{nu} = 10$ ms |

*Mossy fiber input parameters*

| | |
|---|---|
| FEF → mfret | $w_g(i) = \exp(-(i)^2/4)$ for $-4 \leqslant i \leqslant 4$ |
| Eye position → mfpos | $H(i) = -45 + 9i$ for $0 \leqslant i \leqslant 10$ and $s = 20$ |
| EBNr → mfburst | $w_{bmf} = 0.1$ |

*Nonlinear functions parameters*

| | |
|---|---|
| Mossy fibers | $x_1 = 0\ x_2 = 400\ y_1 = 400$ |
| Granule cells | $x_1 = 250\ x_2 = 400\ y_1 = 100$ |
| Purkinje cells | $x_1 = 0\ x_2 = 400\ y_1 = 400$ |
| Nuclear cells | $x_1 = 0\ x_2 = 600\ y_1 = 600$ |

*Constant synaptic weights for the cerebellum*

| | |
|---|---|
| Mossy fibers → GC | $w_{mf\,gc} = 1$ |
| EBNr → FOR | $w_{mn} = 0.3$ |
| PC → FOR neurons | $w_{pn} = 1.5$ |
| FOR → EBNt and IBN | $w_{ne} = 1$ |

*Modifiable weights and eligibility parameters*

| | |
|---|---|
| LTD weight upper bound | $w_{max} = 0.001$ |
| Eligibility parameter | $l_1 = 0.07, l_2 = 0.1$ |
| Eligibility input gain | $K = 10$ |
| Learning rate | $\alpha = 0.0001$ |

*Inferior olive parameters*

| | |
|---|---|
| IO neuron time constant | $\tau_{io} = 30$ ms |
| Spike duration | $\partial = 5$ ms |
| Hyperpolarization parameter | $hyper = 1$ |
| Threshold | $\theta = 0.2$ |

*Other parameters*

| | |
|---|---|
| PC background firing | $B_{pc} = 20$ |
| Width of step function (equation 7 in Schweighofer 1996) | 100 spikes/s |
| FOR background firing | $B_{nu} = 100$ |
| Muscle nonlinearity | $a = 50$ |
| Muscle activation gain | $G = 100$ |
| Muscle linear parameters | $k = 0.37$ and $l = 56$ |
| Max. burst mossy fiber firing | mfburst max = 120 spikes/s |
| 'Memory' cell time const | $\tau_m = 0.1$ s |

*Notes*

The muscle nonlinearity parameter was chosen so that the nonlinearity was significant for large saccades and to match the saccade model (Dominey 1993). Moreover, before performing any experiments, we generated the random connections and the random weights of the model as described in Schweighofer et al. (1996).

The mossy fiber time constant is the same for all mossy fiber types and has been arbitrarily set to an average value. The time constants are taken from Bartha (1993).

The mossy fiber input parameters were chosen so that the generalization across different neighbor targets and positions was significant. Unfortunately, data concerning the extent of the generalization are unavailable at present. Moreover, the position cells respond best between $-45°$ and $+45°$.

The cerebellar weight values were selected to reproduce known FOR firing rates (Fuchs et al. 1993), given the imposed input duration given by the D&A model, the time constants and the number of synapses.

At $t = 0$ for the first trial, the LTD weights are randomly distributed between 0 and $w_{max}$. The eligibility values $l_1$ and $l_2$ were selected so that the time window reaches its peak when the IO spike is generated, to allow more efficient learning. $K$ and $\alpha$ were adjusted so that the learning curve matches somewhat the experimental learning curve given by Goldberg et al. (1993). The IO background firing rate was chosen such that, with the threshold, the average firing rate was 1 Hz. These values were chosen so that the IO fires at a low firing rate in order to match neurophysiological recordings (Bartha 1993). As precise modeling of the IO neurons is outside the scope of the present paper we do not try to reproduce precisely the membrane potential.

*Acknowledgements.* This research was supported in part by grant NOOO14-92-J-4026 from the Office of Naval Research for research on 'Cerebellum and the Adaptive Coordination of Movement'. We thank Dr. M. Goldberg for helping to pose the problem and Dr. W. T. Thach for his comments on an earlier draft. We also thank Dr. M. Kawato and Dr. A. Fagg for their helpful comments.

## References

Bartha G (1993) A computer model of oculomotor and neural contributions to conditioned blink timing. PhD thesis, University of Southern California

Dominey (1993) Models of spatial accuracy and conditional behavior in oculomotor control. PhD thesis, University of Southern California

Dominey P, Arbib M (1992) A cortico-subcortical model for generation of spatially accurate sequential saccades. Cerebral Cortex 2: 153–175

Fuchs AF, Robinson FR, Straube A (1993) Role of the fastigial nucleus in saccade generation: neuronal discharge patterns. J Neurophysiol 70:1723–1740

Gilbert P, Thach WT (1977) Purkinje cell activity during motor learning. Brain Res 128:309–328

Goldberg ME, Musils S, Fitzgibbon E, Smith M, Olson C (1993) The role of the cerebellum in the control of saccadic eye movements. In: Mano N, Hamada I, Delong MR (eds) The role of the cerebellum and basal ganglia in voluntary movement. Excerpta Medica, Amsterdam, pp 203–211

Houk JC, Galiana HL, Guitton D (1992) Cooperative control of gaze by the superior colliculus, brainstem and cerebellum. In: Stelmach GE, Requin J (eds) Tutorials in motor behavior II. Elsevier, Amsterdam

Kase M, Miller DC, Noda H (1980) Discharges of Purkinje cells and mossy fibers in the cerebellar vermis of the monkey during saccadic eye movements and fixation. J Physiol (Lond) 300:539–555

Lewis RF, Zee DS (1993) Oculomotor disorders associated with cerebellar lesions: pathophysiology and topical localization. Rev Neurol (Paris) 149:665–677

McElligot JG, Keller EL (1982) Neuronal discharge in the posterior cerebellum: its relationship to saccadic eye movement generation. In: Lennerstrand G, Zee DS (eds) Functional basis of ocular mobility disorders. Pergamon Press, Oxford

Ohtsuka K, Noda H (1990) Direction-selective saccadic-burst neurons in the fastigial oculomotor region of the macaque. Exp Brain Res 81:659–662

Schweighofer N, Arbib MA, Dominey PF (1996) A model of the cerebellum in adaptive control of saccadic gain. I. The model and its biological substrate. Biol Cybern 75:19–28

Weitzenfeld A (1991) NSL Neural Simulation Language, version 2.1. Technical report 91-02, Center for Neural Engineering, University of Southern California